13th ewtec 2019 Proceedings of the 13th European Wave and Tidal Energy Conference 1-6 Sept 2019, Naples, Italy

Wave energy resource classification system as characterization and assessment tool: Application to the US coast

Kevin A. Haas, Seongho Ahn, and Vincent S. Neary

Abstract— **Energy resource classification systems are useful assessment tools, supporting energy planning and project development, e.g., siting and feasibility studies. They typically establish standard classes of power, a measure of the opportunity for energy resource capture. In this study, we develop wave energy resource classification systems based on wave power (J, kW/m) and its distribution with peak period (T_p, s). These metrics are calculated from partitioned bulk wave parameters generated from a validated 30-year WaveWatch III model hindcast. The classification systems, comprised of four power classes and three peak period band classes, are based on the total wave power or the partitioned wave power in the dominant peak period band. They provide useful information for a variety of stakeholders including energy planners, project developers, and technology designers. Further characterization is done by calculating the attributes of wave energy resource: spectral width, energy-weighted period, directionality coefficient, inter-annual variability, and monthly variability. As an example application for the United States coastal waters, computed marginal and joint energy distributions of the wave resources energy in terms of the peak period, wave direction and month and corresponding resource attributes are compared for two different wave climate regions.**

Keywords—**Wave resource, assessment, characterization, classification**

I. Introduction

OCEAN waves are a largely abundant and untapped renewable source of energy and wave power is considered as a tremendous potential source with limited environmental impact and high energy density [1]. To understand their potential, wave energy resources are often estimated by the theoretical, technical and practical resource [2]. The theoretical resource is an estimate of the amount of energy that is present in the natural sea and the technical resource provides the amount of the theoretical resource that can be technically captured by using a specified technology. The practical resource is the portion of technical resource further constrained by environmental, social, and economic filters [3]. The Electric Power Research Institute (EPRI) and U.S Department of Energy reported that the total theoretical wave energy along the US continental shelf edge is approximately 2,640 TWh/year [4] which is roughly equal to 65% of the annual electricity consumption of the US, 4,054 TWh/year [2]. Although wave power has significant energy potential, wave power is still in the early stages of development due to its high costs from uncertainties in conversion efficiencies, risks to operations, maintenance and survival [5]. One fundamental reason for the high costs is that comprehensive data on theoretical wave energy, and of sufficient quality, is not broadly available to fully inform the development of wave energy conversion technologies [6].

In this study, the wave data from a 30 year hindcast used to develop a wave energy resource classification scheme based on the annual available energy (AAE) and the dominant period band containing the largest energy content is further used to develop secondary attributes to characterize the quality of the energy resource. Many of these parameters are related to those proposed in the International Electrotechnical Commission (IEC) resource assessment technical specification to characterize wave energy resources [7]. Previous studies have adopted these parameters for characterizing regional wave climates [8]–[10]. [8] characterized wave energy resource of the US Pacific Northwest using spectral records from ten buoys. [9] characterized wave energy resource along the continental shelf contours in Oregon and southwest Washington, US using a 7- year hindcast from numerical models (WAVEWATCH III, SWAN). [10] characterized wave energy resource at eight U.S. wave energy converter (WEC) test and potential deployment sites using SWAN hindcasts. Most of the previous studies mainly focused on the regional characterizations with a limited location.

Paper ID Number: 1658; Conference Track: WRC

K. A. Haas (corresponding author), Associate Professor, School of Civil & Environmental Engineering, 790 Atlantic Drive, Georgia Institute of Technology, Atlanta, GA 30332 U.S.A. (e-mail: khaas@gatech.edu).

S. Ahn, Ph.D. Student, School of Civil & Environmental Engineering, 790 Atlantic Drive, Georgia Institute of Technology, Atlanta, GA 30332 U.S.A. (e-mail: seongho.ahn@gatech.edu).

V. S. Neary, Marine energy technologies lead, Water Power Technologies, Sandia National Laboratories, PO Box 5800, Albuquerque, NM 87185 U.S.A (e-mail: vsneary@sandia.gov).

Finally, two examples of detailed characterizations of the wave climate are included to illustrate the value of these attributes for wave resource characterization.

A. Wave data

The wave energy resource attributes are derived using the validated phase II 30-year hindcast from the 3rd generation (3G) spectral wave, WaveWatch III® (WWIII) having a spatial resolution of 4 arc minute [11]. Although frequency-directional wave spectra are internally computed from the model and would be the most comprehensive source of data, limited grid points are retained due to storage limitations. Therefore, hourly spectral partitioned wave parameters, one of the model results, spanning thirty years from 1980 to 2009 at 77,346 grid points along the US coastal waters are used in this study. The partition data are derived using an algorithm initially developed for watershed identification [12], [13] where the frequency-directional wave spectrum is divided into partitions representing energy from sub-peaks within the spectrum. WWIII provides quantitative spectral partition parameters, e.g., partition wave height (H), partition peak period (T_p), partition mean direction (θ), and partition wind-sea fraction [11], [14]. The validation of the model data based on the methods recommended by the IEC technical specification on wave energy resource assessments [11] can be found in [15].

B. Wave resource characterizations

The International Electrotechnical Commission (IEC) recommends the computation of six parameters for characterizing the wave energy resource: omnidirectional wave power (J_i), significant wave height H_{m0}, energy period T_e, spectral width ϵ_0, direction of maximum directionally resolved wave power θ, and the directionality coefficient d [11]. While these are important metrics to consider when characterizing and assessing the wave energy resource, they are computed directly from the wave spectrum; therefore, we propose other metrics that are analogous, but are computed from the partition data. This also has the advantage of separating the various components of the spectrum with individual parameters, such as splitting swell from wind seas.

The hourly wave data is used to compute the wave power (J_i) in kilowatts per unit wave crest length for each i^{th} partition using

$$J_i = \frac{\rho g}{16} {H_i}^2 C_{g\_i} \tag{1}$$

where ρ is the sea water density (1,025 kg/m^3), g is the gravitational acceleration, and C_{g_i} is the group velocity computed using the partition period and depth.

In order to assess not only the total wave power density itself, but also the characteristics of the wave energy, monthly and inter-annual distributions of the partitioned wave power density are quantified in terms of wave direction bins (resolution of 10° clockwise from true North) and peak period bins (resolution of 1s). The 30-year averaged wave power density, $J(T_p, \theta, M, Y)$ is computed as the summation of J_i pairs in the cell (T_p, θ, M, Y) divided by the number of hours in 30-year (T) as

$$J(T_p, \theta, M, Y) = \sum_1^n J_i / T \tag{2}$$

where n is the number of J_i pairs in the cell (T_p, θ, M, Y), M is the month, and Y is the year.

The AAE density in MWh/m, analogous to annual energy production (AEP) without considering the energy conversion process, is calculated. It can be thought of as the theoretical available annual wave energy for any particular location.

$$AAE(T_p, \theta, M, Y) = T_{year} \cdot J(T_p, \theta, M, Y) \tag{3}$$

where T_{year} is the number of hours in a year taken to be 8,766 hours. The AAE density as a function of any parameters, e.g., $AAE(T_p)$, $AAE(\theta, M)$ is taken as the summation over the other parameters. The 30-year averaged total AAE is simply the sum of all components.

As the efficiency of wave energy capture can be maximized by resonating close to the incident wave peak period, wave energy potential can be constrained by the technology operational period bandwidth. Therefore, the frequency dependence of the wave energy is vitally important and the period band containing the largest energy content is identified. In this study, two attributes, AAE-weighted period and spectral width are computed to describe the frequency dependence of the wave energy. These attributes play a large role driving selections of a WEC's operating period bandwidth and the WEC's optimal design size.

The AAE-weighted period is analogous to the energy period (T_e). This attribute indicates the period bandwidth containing the largest energy and is computed as

$$T_{AAE} = \frac{\sum T_p \cdot AAE(T_p)}{AAE} \tag{4}$$

To evaluate the relative range of periods containing significant energy, the relative spreading of the AAE density along the peak period is calculated as the standard deviation of $AAE(T_p)$, normalized by the AAE-weighted period. A small value indicates a narrow frequency spread.

$$\epsilon_{AAE} = \sqrt{\frac{\sum {T_p}^2 \cdot AAE(T_p)}{AAE} - {T_{AAE}}^2} \Big/ T_{AAE} \tag{5}$$

As many WEC technologies can only capture the energy contained within a narrow band of wave directions by

aligning normal to the predominant wave direction, the directional variability of the wave energy may also be important. In order to characterize the directional variability, the directionally resolved AAE density, $AAE(\alpha)$ passing through a vertical plane with normal vector in direction α, is calculated by adding each component of the $AAE(\theta)$ resolved in direction α. The parameter α has a resolution of 10° ranging from 0° to 180° clockwise from true North.

$$AAE(\alpha) = \sum AAE(\theta)|cos(\alpha - \theta)| \tag{6}$$

To characterize the directional spreading of AAE density, the directionality coefficient d_α, the ratio of the maximum directionally resolved AAE density to the total AAE density, is calculated as

$$d_\alpha = \frac{\max[AAE(\alpha)]}{AAE} \tag{7}$$

Larger values indicate less directional spread of the energy.

Another important factor to characterize the wave energy is the temporal variability for different time scales. Computing the temporal variability of the wave energy allows WEC developers to identify sites where the energy is spread more broadly throughout the year, a desirable resource attribute, as opposed to sites where the energy is concentrated within a particular season or year. The temporal variability index has been proposed using different time scales; daily, monthly, seasonally and inter-annually [16]–[18]. In this study, inter-annual variability and monthly variability are calculated.

The monthly variability, MV indicates the maximum range of monthly mean energy relative to the yearly mean value [16].

$$MV = \frac{AAE(M)_{max} - AAE(M)_{min}}{AAE} \tag{8}$$

Where $AAE(M)_{max}$ is the mean AAE density for the most energetic month and $AAE(M)_{min}$ is the mean AAE density for the least energetic month. A large MV indicates that the wave energy has significant variability throughout the year.

TABLE II
DEFINITION OF PEAK PERIOD BAND CLASSES

Class	I	II	III	IV
J (kW/m)	22.8 < J	5.7 < J < 22.8	1.1 < J < 5.7	J<1.1
AAE (MWh/m)	200<AAE	50<AAE<200	10 < AAE < 50	AAE<10

Finally, to examine inter-annual variation, the coefficient of variation, COV is calculated from the $AAE(Y)$. To take into account the actual cyclical variations of the inter-annual wave energy, a linear trend of the $AAE(Y)$ is removed using a regression technique and the COV is calculated as a standard deviation of detrended $AAE(Y)$, divided by the 30-year mean AAE.

$$COV = \frac{\sigma[AAE(Y)_{detrend}]}{AAE} \times 100\ \% \tag{9}$$

Where σ denotes the standard deviation.

C. *Wave resource classification definitions*

The wave resource classification system was presented in [12]. Because the operating resonant period bandwidth of a wave energy converter (WEC) technology is an important design characteristic, the wave power and AAE partition data is split into three different period bands defined in Table I. These peak period bands are designed to discriminate different WEC operating bandwidths, but they roughly correspond to peak period bands for regionally dominant energy transfer by local wind seas, short period swell or long period swell.

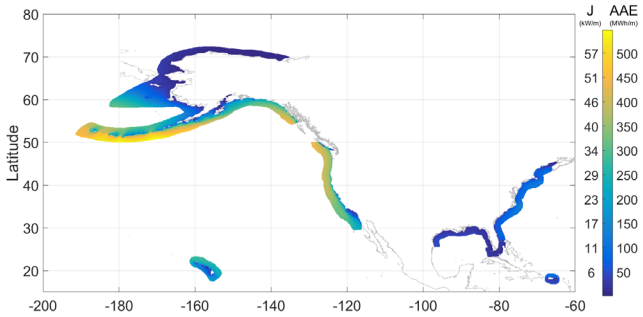

TABLE I
DEFINITION OF PEAK PERIOD BAND CLASSES

Class	Band 1	Band 2	Band 3
Period $T_p(s)$	$0 < T_p < 7$	$7 < T_p < 10$	$T_p > 10$

Four wave power classes are defined as shown in Table II. The delineation of power classes I-IV is adjusted to discern the distinct geo-spatial regional resource trends for US coastal waters. The threshold value separating classes II and III corresponds approximately to the median wave power density computed for the US (5.7 kW/m). The threshold between I and II (22.8 kW/m) is set one standard deviation higher than the mean value (12.0 kW/m), and that between III and IV (1.1 kW/m) one standard deviation lower than the mean value.

II. RESULTS

D. *Wave resource classification*

The geographical distribution of the total AAE density along the US coastal waters is shown in Fig 1. The wave energy distribution is generally consistent with results from previous studies [4], [6]. As expected, the wave energy offshore is more energetic than nearshore. The largest energy, with AAE densities exceeding 400 MWh/m, is found along the Cascadia subduction zone located at Pacific Northwest coast and along the Aleutian Trench. The California coast near the San Andreas Fault has

moderate energy compare to the Pacific Northwest coast, on the order of 300 MWh/m. Hawaii has slightly lower energy potential compared to the West coast, on the order of 200 MWh/m. The wave energy potential at the East coast and Atlantic Ocean side of Puerto Rico is typically below 100 MWh/m. The smallest energy, with AAE densities below 50 MWh/m, along the US coast waters except for arctic Alaska is found the Gulf of Mexico and Caribbean Sea side of Puerto Rico.

While the geographic variation in AAE for the US coastal waters is useful for evaluating the relative energy potential for various regions, it is beneficial to distill it down to the essentials by incorporating the wave resource classification system. Two classification systems were considered: one based on the total wave power (herein referred to as the Total Power Class) and the other based on the maximum wave power occurring in the dominant peak period band (herein referred to as the Max Band Power Class). The total wave power or band wave power determines the power class (I-IV), and the predominant period band containing the largest energy content determines the subclass (1-3).

As an example, the geographical distribution of the Max Band Power Class in Fig. 2 to delineate distinct regional patterns of dominant resource classes. Class I(3) resource sites are exclusive to the West Coast region, along the

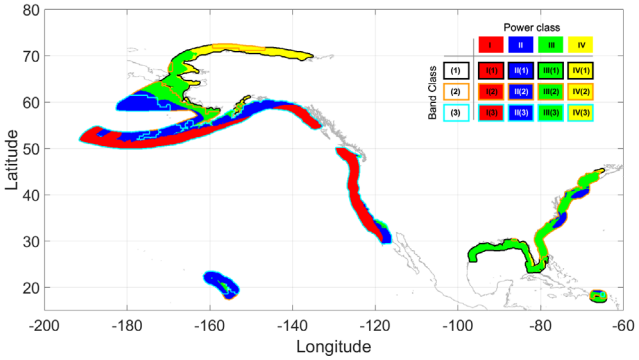

Fig. 2. Geographical distribution of Max Band Power Classification system (similar to results shown in [12]). The face color indicates the class of the wave power in the predominant peak period band and edge color indicates the class of predominant period band.

southern coast of Alaska, and a small region in northern Hawaii. The Total Power Class I(3) sites offshore of the west coast of Alaska in the Bering Sea at approximately sixty-degrees latitude, and most of the I(3) sites in Hawaii, become Max Band Power Class II(2) and Class II(3) sites. Likewise, most of the Total Power Class II sites on the East Coast cannot qualify as Max Band Power Class II sites, demoting to Class III(2) sites.

E. Wave resource characterization

As described in section B, a number of parameters can be computed to better characterize the resource beyond just the available power. These parameters can be thought of as a way of characterizing the quality of the power. The relevance of each parameter will depend on the particular WEC technology being considered. These parameters may

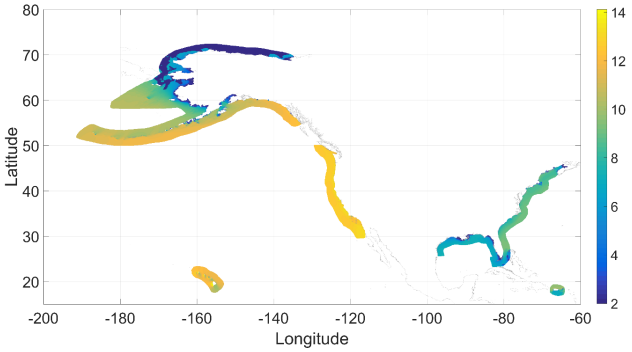

Fig. 3. Geographic distribution of the energy-weighted period in seconds, computed with (4).

also be used to determine what type of device would be most optimal for the wave resource conditions.

Because of the importance of the frequency dependence of the WEC technologies, the energy-weighted period, T_{AAE} and the spectral width, ϵ_{AAE} indicating the period bandwidth containing largest energy is identified. The geographical distribution of the energy-weighted period and the spectral width along the US coastal waters is shown in Fig. 3 and 4, respectively.

Interestingly, similar to the distribution of the total AAE density, the frequency dependence is roughly grouped by the different regions as shown in Fig. 3. Generally, long period swells ranging from 10 to 14s contain the largest

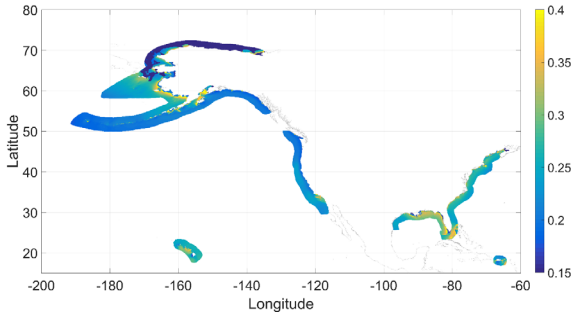

Fig. 4. Geographic distribution of the spectral width ϵ_{AAE}, computed with (5). A small value indicates a narrow frequency spread.

energy for the Pacific Ocean coast and intermediate period swell ranging from 8 to 10s contain the largest energy for the Atlantic Ocean coast. In the Gulf of Mexico coast, relatively short period wave systems, less than 8s, have the largest energy. These period regimes roughly correspond to long period swell and relatively short period swell and local wind sea. The California coast has the largest T_{AAE} among the US coastal waters, requiring WEC technologies deployed here to be sufficiently large to achieve resonance for optimal energy capture.

As shown in Fig. 4, the spectral width varies from 0.15~0.4 along the US coastal waters; the east coast of the Gulf of Mexico and Florida Straits have the largest values exceeding 0.3. The Pacific Ocean coast generally has a narrow spectral width compare to the Atlantic Ocean coast, except the Hawaiian coast where the energy is distributed into two separate frequency peaks leading a relatively large spectral spreading. Along the Hawaiian

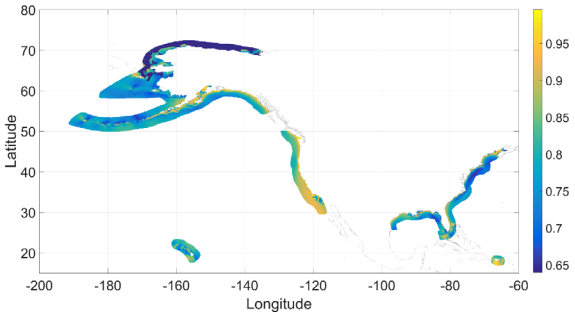

Fig. 5. Geographic distribution of the directionality coefficient computed with (7). Larger values indicate less directional spread of the energy.

coast, a narrow operating frequency bandwidth of the WEC technologies may constrain the ability to capture a large amount of energy contained in the other peak. Interestingly, the Puerto Rico coast has a relatively narrow spectral width compare to the other portions of the Atlantic coast. For the West coast, the Pacific Northwest has a more narrow spectral width compared to California.

While the spectral width and energy-weighted period describe the frequency sensitivity of the wave energy, the directionality coefficient indicates the directional variability. The geographical distribution of the directionality coefficient is shown in Fig. 5. Unlike the AAE density, where the waves in the offshore region have higher values than in the nearshore, the waves in the nearshore generally tend to have a higher directionality coefficient than in the offshore. This result is consistent with wave refraction where the waves tend to become more shore normal as they approach the shore.

Overall, the directionality coefficient along the nearshore is generally above 0.9. Further offshore the value ranges from 0.7 to 0.9 except off the California coast and the Caribbean Sea side of Puerto Rico. Interestingly, they have relatively high coefficients exceeding 0.9, indicating that the wave systems in this area have a narrow directional spread. As the waves in these regions are

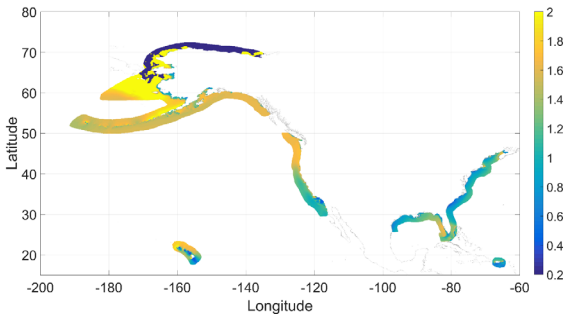

Fig. 6. Geographic distribution of the monthly variability computed with (8). A large MV indicates that the wave energy has significant variability throughout the year.

directionally focused, the complexities and costs of weather-vaning directionally-dependent WEC technologies, e.g., attenuators, and even omnidirectional WEC farms, can be reduced. Unusually, the waves in the nearshore have a smaller coefficient than in the offshore along the Atlantic Continental Slope and eastern Gulf of Mexico (Florida Shelter). This happens when the alongshore waves generated by local winds propagate over the steep slope which is perpendicular to the wave rays.

Another factor that must be considered when evaluating potential locations for wave energy is the temporal variability of the wave climate. The seasonal variability may lead to inconsistent power during the year. The geographical distribution of the monthly variability is shown in Fig. 6. The Pacific coast generally has a large value of monthly variation compared to the Atlantic coast and the Gulf of Mexico. In the nearshore arctic regions, the

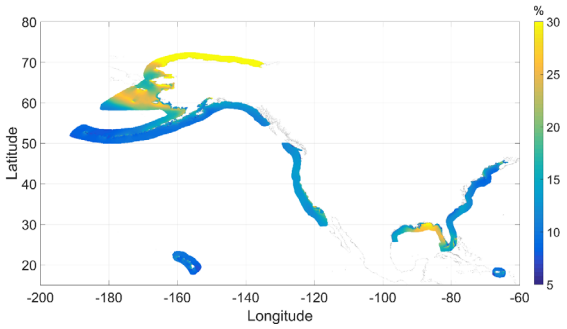

Fig. 7. Geographic distribution of the inter-annual variability computed with (9). A large COV indicates that the wave energy has significant year to year variability.

MV is significantly large due to the effects of intermittent ice cover. The largest MV outside the arctic regions, on the order of 1.5, generally occur in Pacific Northwest coast, the southern coast of Alaska and the northern coast of Hawaii which means that the maximum range in monthly mean available energy is 1.5 times greater than AAE in these regions. The eastern Gulf of Mexico also has a large value due to the extreme events. Interestingly, the California coast has a relatively small monthly variation compared to the Pacific Northwest coast, on the order of 1.0.

In additional to seasonal or monthly variability, the wave resource may have inter-annual variability. The geographical distribution of the inter-annual variability of the wave energy is shown in Fig. 7 as the COV of the detrended AAE density over the 30-year period. The COV represents the irregular inter-annual fluctuations of the wave energy driven by the El Niño Southern Oscillation (ENSO) which provides a steady source of baroclinic instability leading to convective energy. The largest oscillations occur at the Bering Sea below the Alaska artic area and the central-eastern Gulf of Mexico exceeding 25%. Inter-annual variabilities of air, ocean and ice parameters at the Bering Sea has a strong cross-correlation with the southern correlation index (SOI), an index of ENSO [19]. The stronger influence of the subtropical jet stream generated by typical ENSO events impacts for the Southeast US, especially in the Gulf of Mexico coast [20]. The Hawaiian coast has a relatively small inter-annual variability among the US coastal waters below 10%.

F. Wave resource regional characterization

The previous section discussed broad wave energy characterizations, focusing on parameters that indicate the potential quality of the resource. This section demonstrates the regional wave energy potential by providing averaged marginal distributions of the wave energy potential in terms of the peak period, direction and month. In addition, reliability attributes, spectral width, directional spread, temporal variability of the resolved wave energy potential are characterized for each region. Finally, the portion of the energetic wave systems contributing to the total wave energy for each region is identified and characterized by providing the joint energy distributions and linking to the wind climatology. As an example, two regions in US coastal waters are included here, the Pacific Northwest and the northern coast of Hawaii.

Given the importance of period, directional and temporal variabilities on the operation of WEC technologies, descriptions of the wave energy potential, AAE density, and other resource attributes as a function of peak period, direction and month are useful. In order to gain unique wave energy resource characteristics, regional joint distributions giving the wave energy potentialities for any subset of the parameters conditional on particular values of the remaining parameters are presented in Fig. 8 and Fig. 9.

The joint distributions, $AAE(T_p, \theta, M)$, for all the locations within a region are averaged together to create the averaged regional joint distribution. These results illustrate how much wave energy potential is found for each sea state (AAE as a function of peak period and direction) as a function of the monthly temporal variation along with all interdependencies. The attributes which

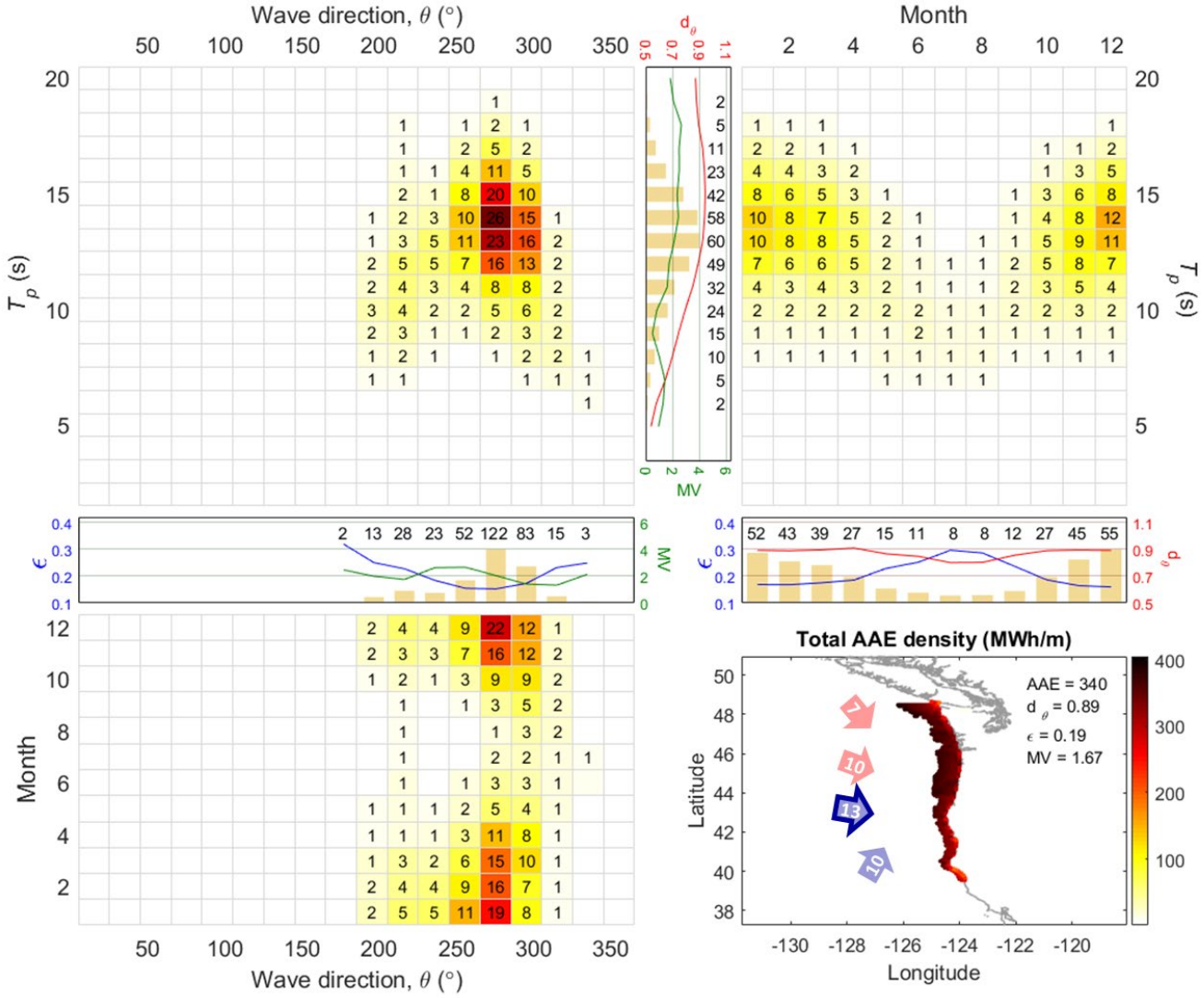

Fig. 8. Pacific Northwest coast, averaged joint distributions, $AAE(T_p, \theta)$ (top, left), $AAE(T_p, M)$ (top, right), $AAE(M, \theta)$ (bottom, left) and averaged marginal distributions, $AAE(T_p)$, $AAE(\theta)$, $AAE(M)$ with corresponding resource attributes, d_α (red line), MV (green line), ϵ (blue line), and geographical distribution of the total AAE density (bottom, right). Resolutions of T_p, θ and M distributions are 1s, 20° clockwise from the true north and month, respectively. The numerals and colors in the joint and marginal distributions indicate the averaged AAE density within particular wave systems. The arrows in the geographical distribution show energetic wave systems indicating the direction, peak period (numeral) and season (red: summer, blue: winter, grey: all year round) of each system. The arrow with bold edge indicates the most energetic wave system. The average of total AAE density and d_α, MV, ϵ of the total AAE density is also shown in the geographical distribution.

serve as resource variability indices for each site, $d_\alpha(T_p)$, $MV(T_p)$, $\epsilon(\theta)$, $MV(\theta)$, $d_\alpha(M)$, and $\epsilon(M)$ are calculated using the marginal distributions of the AAE density, $AAE(T_p)$, $AAE(\theta)$ and $AAE(m)$. In addition, the sources of energetic wave systems are described by linking the local and global wind climatology, Scatterometer Climatology of Ocean Winds (SCOW) based on 10 years of QuikSCAT scatterometer data [21], [22].

The Pacific Northwest coast is illustrated in Fig. 10. The total AAE density tends to increase along the increasing latitude with energetic sites mainly located offshore of the Pacific Northwest coast having power approximately 350 MWh/m. The inshore wave energy is smaller but still robust, on the order of 300 MWh/m. The overall spectral width is fairly small and the overall directionality coefficient is fairly large, illustrating a high quality energetic wave system.

Looking in more detail, the local wind-sea (7s) mainly come from NW in summer and short period swells (8-10s) come from SSW in winter and from WNW in summer. Longer period swells (>11s) are mainly generated from W in winter. The marginal distributions show that the long period swell (13-14s), the waves from W and winter contain the most energy, respectively. The d_α in terms of peak period is largest at the energetic period band, long period swell (13-14s), on the order of 0.9. The MV in terms of peak period is remarkably small at the short period swell band (8-10s), on the order of 1.0, due to the two comparable wave systems in both summer and winter. The ϵ in terms of the wave direction has a large fluctuation where the ϵ is smallest at the energetic directional band, on the order of 0.15. The ϵ in terms of the month also has the large fluctuation where the ϵ is small in winter and large in summer. The d_α in terms of the month is relatively small in the summer, on the order of 0.8.

The wave energy distribution in this region has four wave systems; the most energetic wave system (13-14s) coming from W in the winter, the wave system (9-11s) coming from SSW in the winter and WNW in the summer, the wave system (6-7s) with a little energy coming from NW in summer. The energetic swells are driven by westerlies from the WSW toward ENE in the winter. The directions of local wind are seasonally changed. The local winds blow from NNW in summer and from SSW in winter.

This data is also used to evaluate the influence of the resource characteristics on WEC design. The remarkably narrow directional and frequency spreading of the energetic wave systems potentially allows for a simplification of the device design for fewer frequencies/directions, potentially leading to a decrease in the cost of energy in this region. For this region, targeting WEC technologies with an operating period of 13-14s would maximize the energy capture for this region. Because the long period swells contain the most energy, WEC technology in this region will need to be relatively large to achieve natural resonance for optimal energy capture [23].

A second example is included, the northern Hawaiin coast shown in Fig. 11. The energetic sites are again mainly located offshore, on the order of 200 MWh/m. The overall directionality coefficient is relatively small due to two comparable wave systems generated by westerlies and Trade winds. The wave system generated by the westerlies has long periods and the wave system generated by the Trade winds has relatively short periods. For this reason, the overall spectral width is relatively large compared to the other regions located in the Pacific Ocean.

Short period swells (8-10s) mainly come from ENE almost all year round and long period swells (13-15s) mainly come from NW in the winter. The marginal distributions have two comparable peaks in both peak period and wave direction. The d_α and MV as a function of the peak period are large at the long period swells and relatively small at the short period swells. The ϵ in terms of the direction is large at the ENE directional band and small at the NW directional band. On the other hand, the MV in terms of the direction is small at the ENE directional band and large at the NW directional band. The ϵ in terms of the month is small during winter, on the order of 0.2, and large in the summer, on the order of 0.25. The d_α in terms of the month is relatively small in the summer, on the order of 0.7.

This region can be divided into three areas: the west part (Kauai and Niihau), center (Oahu and Maui), east part (Hawaii). As discussed above, the energy distribution in this region has two separate wave systems. Interestingly, sub-areas of this region have a different dominant peak between the two wave systems. The wave system (13-15s) from NW contains the most energy at the west part and the wave system (8-10s) from ENE contains the most energy at the east part. Therefore, the wave energy at the west part is mainly distributed in the winter and has a high value of MV. The wave energy at the east part is distributed throughout the year with relatively low MV. On the other hand, two wave systems equally contribute to the total energy at the center area. The wave system (8-10s) from ENE is generated by the Trade winds and wave system (13-15s) from NW is generated by the westerlies from the WNW traveling a long distance across the Pacific Ocean in winter.

The effect of the wave resource characteristics on the WEC technology varies for different sub-areas. In the western sub-area, an operating period range of 13-15s may be recommended to maximize the energy capture and directionally dependent WEC devices need to face NW. Whereas, in the eastern sub-area, an operating period range of 8-10s may be recommended to maximize the energy capture and directionally dependent WEC devices need to face ENE. WEC technologies. Because of the dominant longer period swell in the western sub-area, the WEC technology deployed there may need to be relatively large compared to the eastern sub-area. In the center sub-

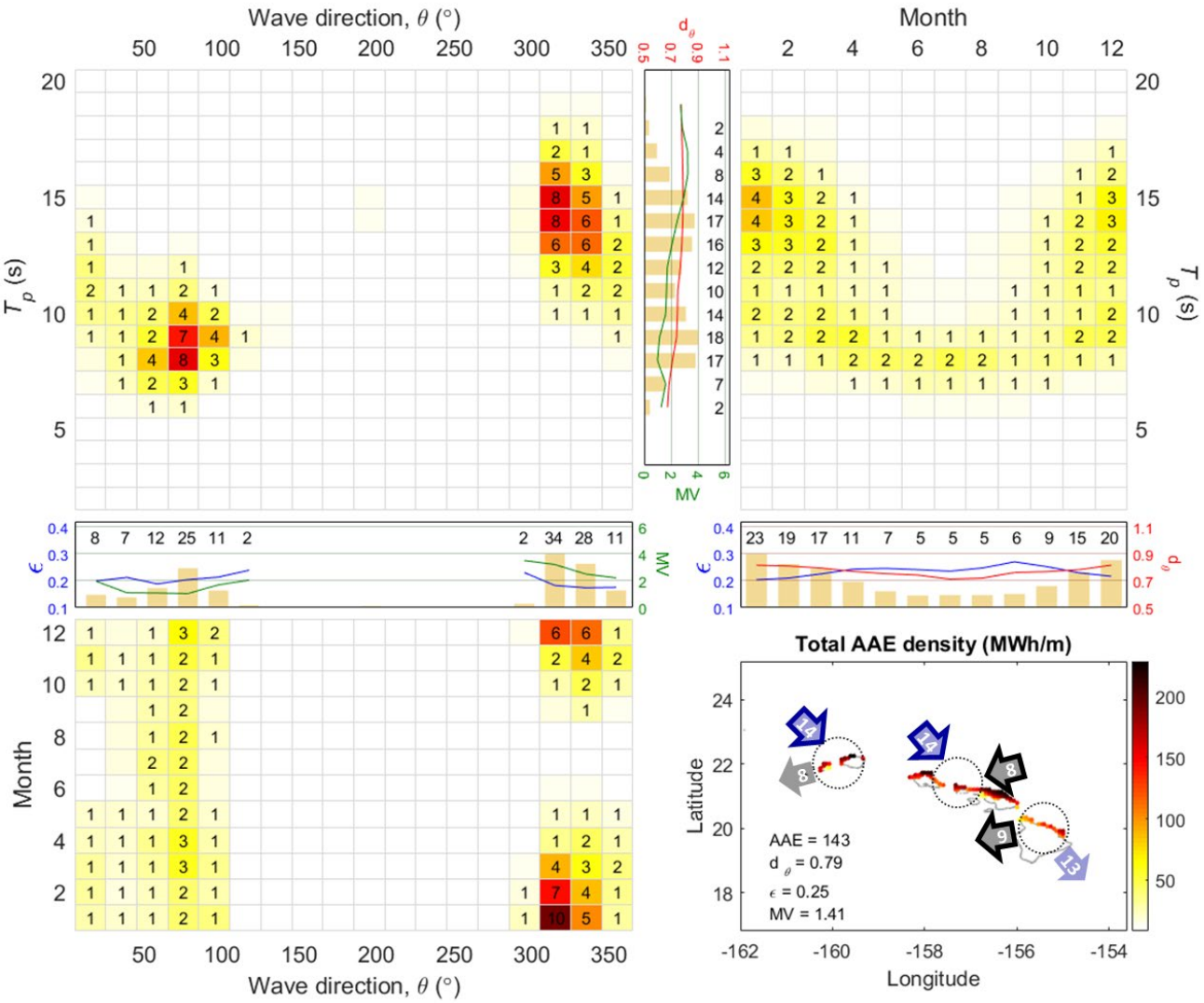

Fig. 9. Northern Hawaii coast, averaged joint distributions, $AAE(T_p, \theta)$(top, left), $AAE(T_p, M)$(top, right), $AAE(M, \theta)$(bottom, left) and averaged marginal distributions, $AAE(T_p)$, $AAE(\theta)$, $AAE(M)$ with corresponding resource attributes, d_α(red line), MV (green line), ϵ(blue line), and geographical distribution of the total AAE density (bottom, right). The detailed descriptions are identical to the Fig. 8.

area, because both types of wave conditions exist with a high level of energy, a wave energy development project will need to select a target wave system based on the pros and cons of the two wave systems.

III. CONCLUSION

The wave energy resource classification system developed for the US based on wave power (J, kW/m) and the dominant peak period band (T_p, s) delineated four wave power classes, representing different wave energy conversion opportunities, and three peak period band classes, representing different wave energy transfer mechanisms, local wind-seas, and short and long-period swell. The benefit for using the distribution of wave power within the peak period bands is to allow WEC project planners and designers to identify sites where energy is concentrated within a dominant period bandwidth, a desirable resource attribute, as opposed to sites where the energy is spread relatively more broadly among multiple period bands.

However, beyond just evaluating the power and dominant period band, the wave data are further analyzed to produce additional characterizations of the quality of the wave resource. The energy weighted period and the spectral width provide a high level of detail about the frequency dependence of the wave climate. Some WEC technologies are better suited for particular frequencies and may be more efficient for narrow spectral widths. Projects that utilize any WEC technology that has a directional dependence benefit from analysis of the directional spread. In order to more reliably provide long term estimates of power production, metrics measuring the seasonal and intra-annual variability in the resource assist the project developers

Depending on the particular technology, developers can use the relevant characterization parameters to help with siting and feasibility assessments. In addition, the WEC technology developers benefit from knowing the range of conditions that potentially exist such that they can target the technology to work most efficiently under those conditions.

ACKNOWLEDGEMENT

The work presented in the paper was supported by Sandia National Laboratories. Sandia National Laboratories is a multi-mission laboratory managed and operated by National Technology and Engineering Solutions of Sandia, LLC., a wholly owned subsidiary of Honeywell International, Inc., for the U.S. Department of Energy's National Nuclear Security Administration under contract DE-NA0003525. This paper describes objective technical results and analysis. Any subjective views or opinions that might be expressed in the paper do not necessarily represent the views of the U.S. Department of Energy or the United States Government. We would like to thank Arun Chawla and NOAA for providing the WWIII hindcast data.

REFERENCES

[1] R. Alamian, R. Shafaghat, M. Safdari, and R. Bayani, "An empirical evaluation of the sea depth e ff ects for various wave characteristics on the performance of a point absorber wave energy converter," *Ocean Eng.*, vol. 137, no. August 2015, pp. 13–21, 2017.

[2] Department of Energy (DOE), "Quadrennial Technology Review 2015, Chapter 4: Advancing Clean Electric Power Technologies, Technology Assessments," 2015.

[3] *An Evaluation of the U.S. Department of Energy's Marine and Hydrokinetic Resource Assessments*. National Academies Press, Washington, D.C., 2013.

[4] S. G. Jacobson PT, Hagerman G, "Mapping and assessment of the United States ocean wave energy resource. EPRI 2011 Technical Report to U.S. Department of Energy," 2011.

[5] C. J., *Ocean wave energy: current status and future perspectives. Green Energy and Technology.* Springer: Berlin., 2008.

[6] A. R. Dallman and V. S. Neary, "Characterization of U.S. Wave Energy Converter (WEC) Test Sites: A Catalogue of Met-Ocean Data," Albuquerque, NM, and Livermore, CA (United States), Oct. 2014.

[7] IEC, "International Standard, Marine energy – Wave, tidal and other water current converters – Part 101: Wave energy resource assessment and characterization, IEC 62600-101: Edition 1.0," 2015.

[8] P. Lenee-bluhm, R. Paasch, and H. T. Özkan-haller, "Characterizing the wave energy resource of the US Paci fi c Northwest," vol. 36, 2011.

[9] G. García-Medina, H. T. Özkan-Haller, and P. Ruggiero, "Wave resource assessment in Oregon and southwest Washington, USA," *Renew. Energy*, vol. 64, pp. 203–214, Apr. 2014.

[10] A. R. Dallman and V. S. Neary, "Characterization of U . S . Wave Energy Converter (WEC) Test Sites®: A Catalogue of Met-Ocean Data 2nd Edition," no. September, 2015.

[11] A. Chawla, D. M. Spindler, and H. L. Tolman, "Validation of a thirty year wave hindcast using the Climate Forecast System Reanalysis winds," *Ocean Model.*, vol. 70, pp. 189–206, Oct. 2013.

[12] J. L. Hanson and R. E. Jensen, "Wave system diagnostics for numerical wave models," in *International Workshop on Wave Hindcasting and Forecasting*, 2004.

[13] L. Vincent and P. Soille, "Watersheds in digital spaces: an efficient algorithm based on immersion simulations," *IEEE Trans. Pattern Anal. Mach. Intell.*, vol. 13, no. 6, pp. 583–598, Jun. 1991.

[14] H. L. Tolman, "User manual and system documentation of WAVEWATCH-III version 3.14," 2009.

[15] S. Ahn, K. A. Haas, and V. S. Neary, "Wave energy resource classification system for US coastal waters," *Renew. Sustain. Energy Rev.*, vol. 104, pp. 54–68, 2019.

[16] A. Cornett, "A global wave energy resource assessment," in *International Offshore and Polar Engineering Conference*, 2008, vol. ISOPE-2008.

[17] B. G. Reguero, I. J. Losada, and F. J. Méndez, "A global wave power resource and its seasonal , interannual and long-term variability," vol. 148, pp. 366–380, 2015.

[18] R. A. Arinaga and K. F. Cheung, "Atlas of global wave energy from 10 years of reanalysis and hindcast data," *Renew. Energy*, vol. 39, no. 1, pp. 49–64, Mar. 2012.

[19] H. J. Niebauer, "Effects of E1 Nino-Southern Oscillation and North Pacific Weather Patterns on Interannual Variability in the Subarctic Bering Sea," vol. 93, pp. 5051–5068, 1988.

[20] A. J. Kennedy, M. L. Griffin, S. L. Morey, S. R. Smith, and J. J. O. Brien, "Effects of El Nin ˜ o – Southern Oscillation on sea level anomalies along the Gulf of Mexico coast," vol. 112, pp. 1–16, 2007.

[21] C. M. Risien and D. B. Chelton, "A Global Climatology of Surface Wind and Wind Stress

Fields from Eight Years of," no. 1989, pp. 2379–2413, 2008.

[22] Craig M. Risien, "The scatterometer Climatology of Ocean Winds (SCOW)," 2011. [Online]. Available: ftp://cioss.coas.oregonstate.edu/pub/scow/.

[23] L. Liberti, A. Carillo, and G. Sannino, "Wave energy resource assessment in the Mediterranean , the Italian perspective," vol. 50, pp. 938–949, 2013.